

C O M P A R A T I V E S T U D Y O F R A D I O A N D O P T I C A L P H O T O M E T R Y O F S E V E R A L H II R E G I O N S . I I

(*CALIBRATION PROCEDURE, AND TABLES OF H_α INTENSITY AND
OPTICAL DEPTH*)

E. F. Schmitter and E. Recillas-Cruz

SUMARIO

En este trabajo se presentan tablas y mapas de contornos de la intensidad y profundidad óptica en H_α para las nebulosas gaseosas NGC 896, NGC 1976, NGC 1982, NGC 2024 e IC 1795. Las observaciones y los resultados han sido publicados recientemente por Schmitter (1971).

También se discuten los detalles del procedimiento seguido en la calibración.

ABSTRACT

This paper presents tables and contour maps of the H_α intensity and optical depth of the gaseous nebulae NGC 896, NGC 1976, NGC 1982, NGC 2024 and IC 1795. The observations and results have been published recently (Schmitter 1971). The calibration procedure is discussed in detail here.

I. Introduction

In earlier investigations values for interstellar extinction in some galactic nebulae are obtained by a comparison between radio and optical isophotes (Schmitter 1971; see also Gebel 1968; Ishida and Kawajiri 1968; Werner, Pipher, Terzian and Houck 1969).

This paper presents details concerning the calibration of the H_α intensity in NGC 896, NGC 1976, NGC 1982, NGC 2024 and IC 1795, published recently (Schmitter, 1971), hereafter referred to as Paper I. Tables of H_α intensity and of optical depth for these H II regions are also given.

II. Microphotometric Work and Calibration

One of us (E. S.) obtained 37 plates using the 26/31 inch Schmidt telescope at the Observatory of Tonantzintla. The scale is 94" per mm. Six of these plates were taken on the same night and were developed together. The latter plates were used in the calibration. A Wratten filter F29 was used in combination with a Kodak 103aE emulsion. The resulting transmission curve is shown in Figure 1.

During each exposure a corner of the plate was covered to reserve it for the calibration spots. These spots were obtained with a sensitometer consisting of a stepped disk rotating very rapidly (1725 rpm). It is expected that in this way the intermittency effect is practically eliminated. The total exposure time of the sensitometer was made equal to the exposure time of the plate.

A few plates for each nebula were traced with a microphotometer in the following way: several constant declination profiles were obtained for each nebula with a circular analyzing beam 90" in diameter. The tracings were spaced by 94". Reference to field stars assure that the equivalent profiles on two or more different plates of the same nebula corresponded to the same position of the strip. These profiles were then superposed onto the radioisophotes. One single profile at a given declination was deemed sufficient for each one of the calibration plates.

The absolute calibration of the set of sensitometric spots on each plate was accomplished by comparison with photoelectric measurements of NGC 1976 in the following way. A density *vs.* absolute intensity curve (open circles in Figure 2) was obtained by plotting the microphotometric measurements on a short exposure plate of Orion against the H_α intensities measured photoelectrically by Méndez (1967). A correction for the contribution of [N II] lines was also applied.

Similarly a density *vs.* relative intensity curve was constructed for the sensitometer spots. By superposing the latter curve on the former one the absolute intensities of the spots were obtained (filled circles in Figure 2).

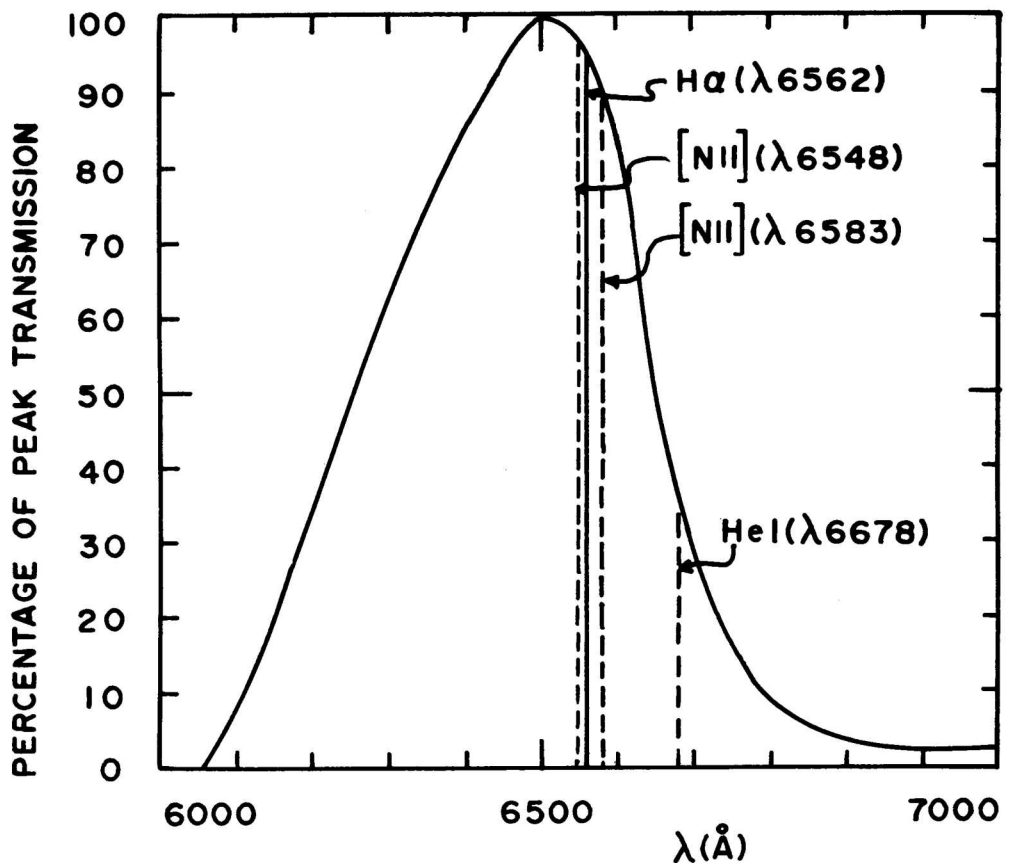


Fig. 1.—Transmission curve of the plate-filter combination.

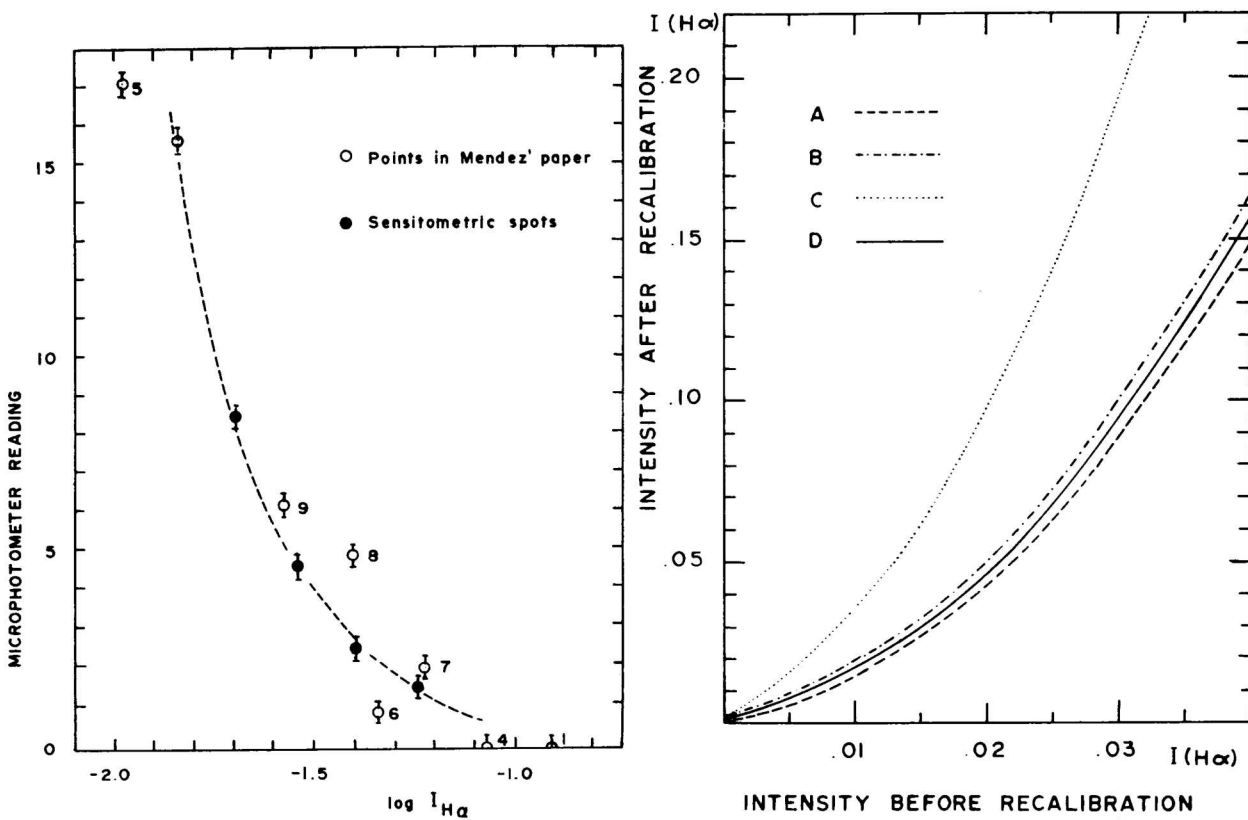


Fig. 2.—First calibration curve. Units of $I_{H\alpha}$ are ($\text{erg cm}^{-2} \text{ sec}^{-1} \text{ sterad}^{-1}$).

Fig. 3.—Recalibration curves plotted with observations made by: A.—Méndez (1967), B.—O'Dell and Hubbard (1965), and C.—Boyce (1966). Recalibration curve D is the one used in this work.

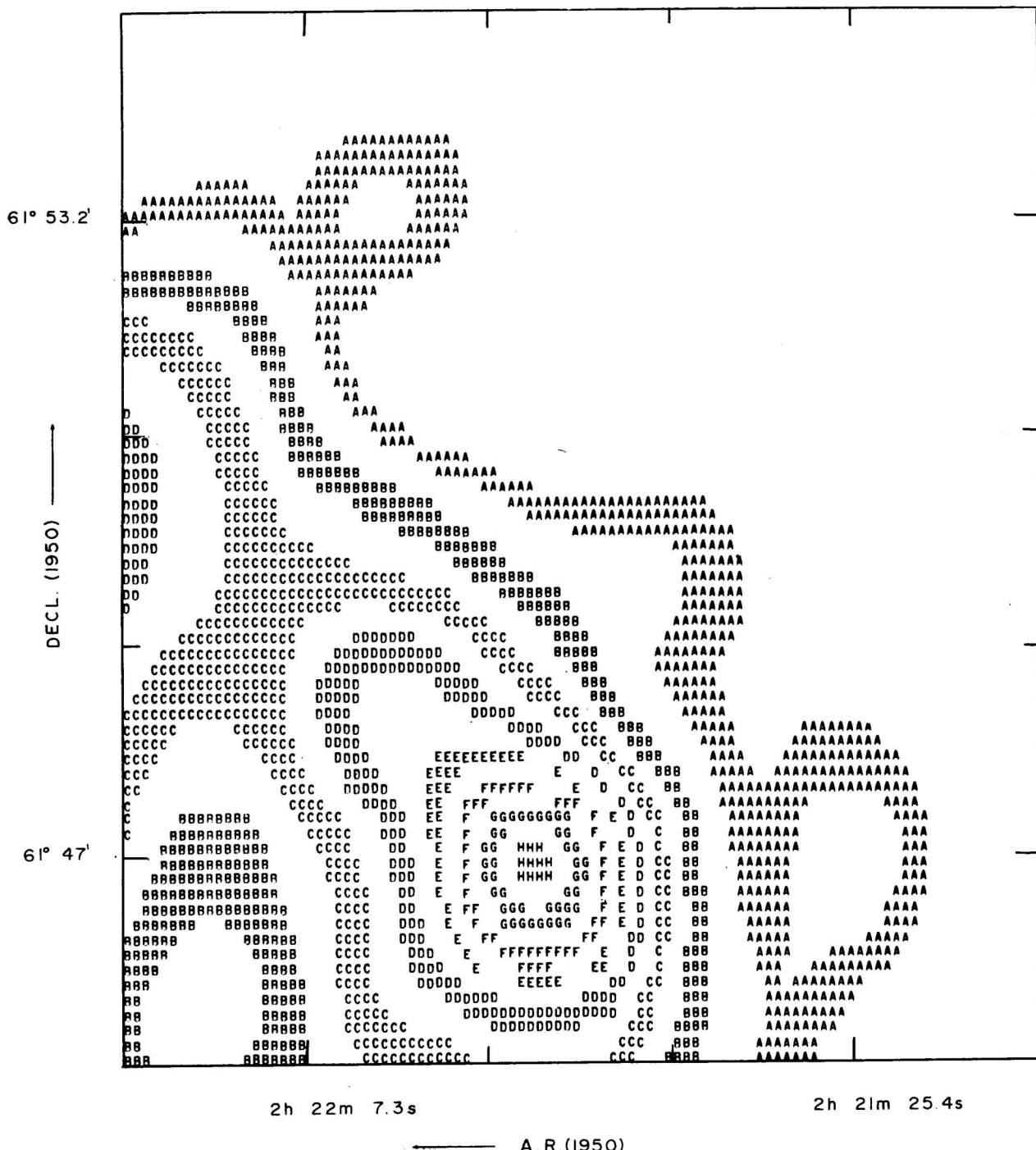


Fig. 4.—Observed intensity contours of NGC 896. Each symbol represents the following range of intensities (10^{-4} erg cm^{-2} sec^{-1} sterad $^{-1}$): $1.216 \leq A \leq 1.491$, $2.010 \leq B \leq 2.539$, $3.069 \leq C \leq 3.598$, $4.127 \leq D \leq 4.656$, $5.185 \leq E \leq 5.450$, $5.979 \leq F \leq 6.508$, $7.038 \leq G \leq 7.567$, $7.831 = H$.

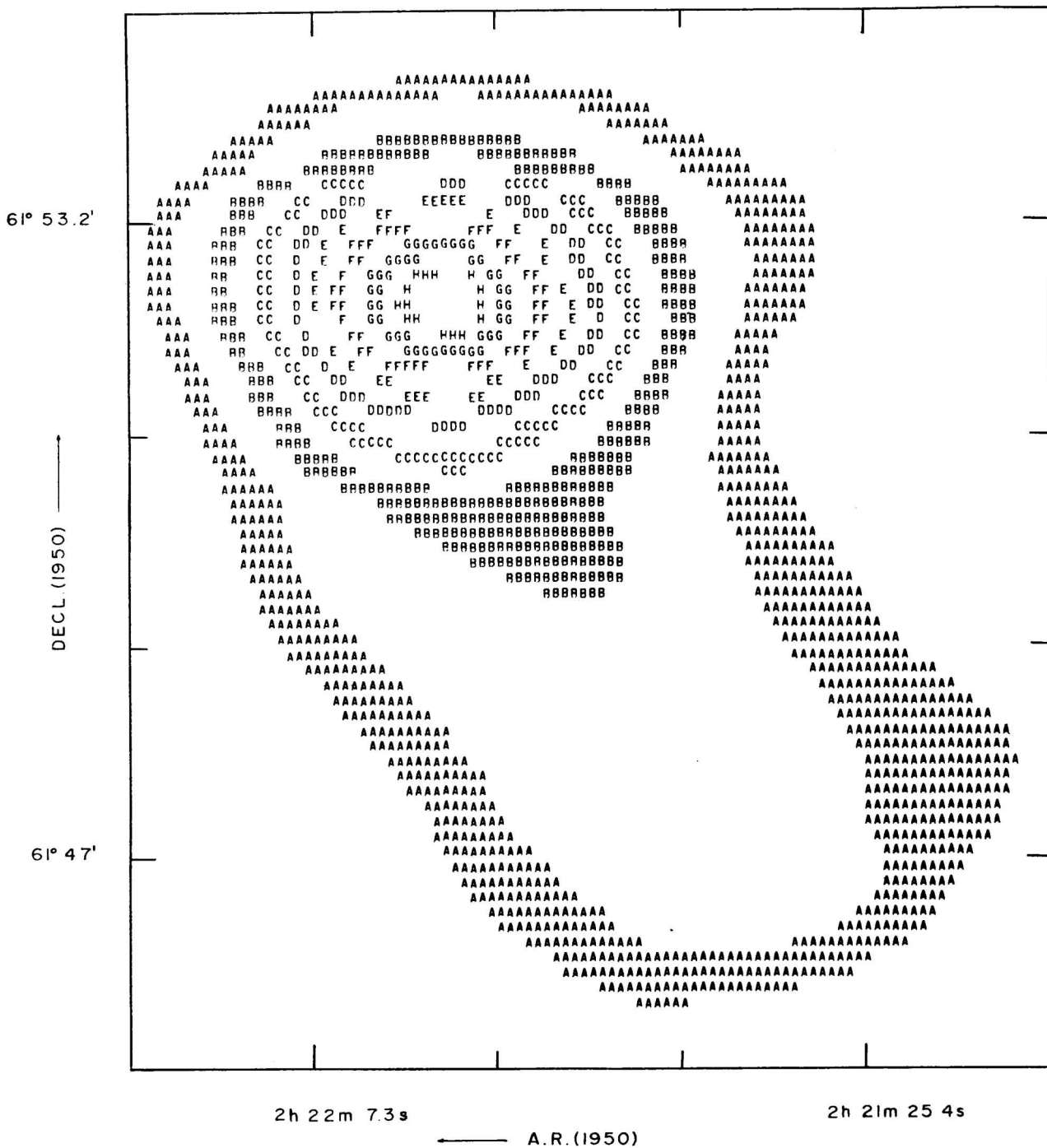


Fig. 5.—Calculated Intensity contours of NGC 896. Each symbol represents the following range of intensities (10^{-2} erg cm^{-2} sec^{-1} sterad $^{-1}$): $0.653 \leq A \leq 0.991$, $1.663 \leq B \leq 2.335$, $3.007 \leq C \leq 3.678$, $4.350 \leq D \leq 5.022$, $5.694 \leq E \leq 6.030$, $6.701 \leq F \leq 7.373$, $8.045 \leq G \leq 8.717$, $9.053 \leq H \leq 9.389$.

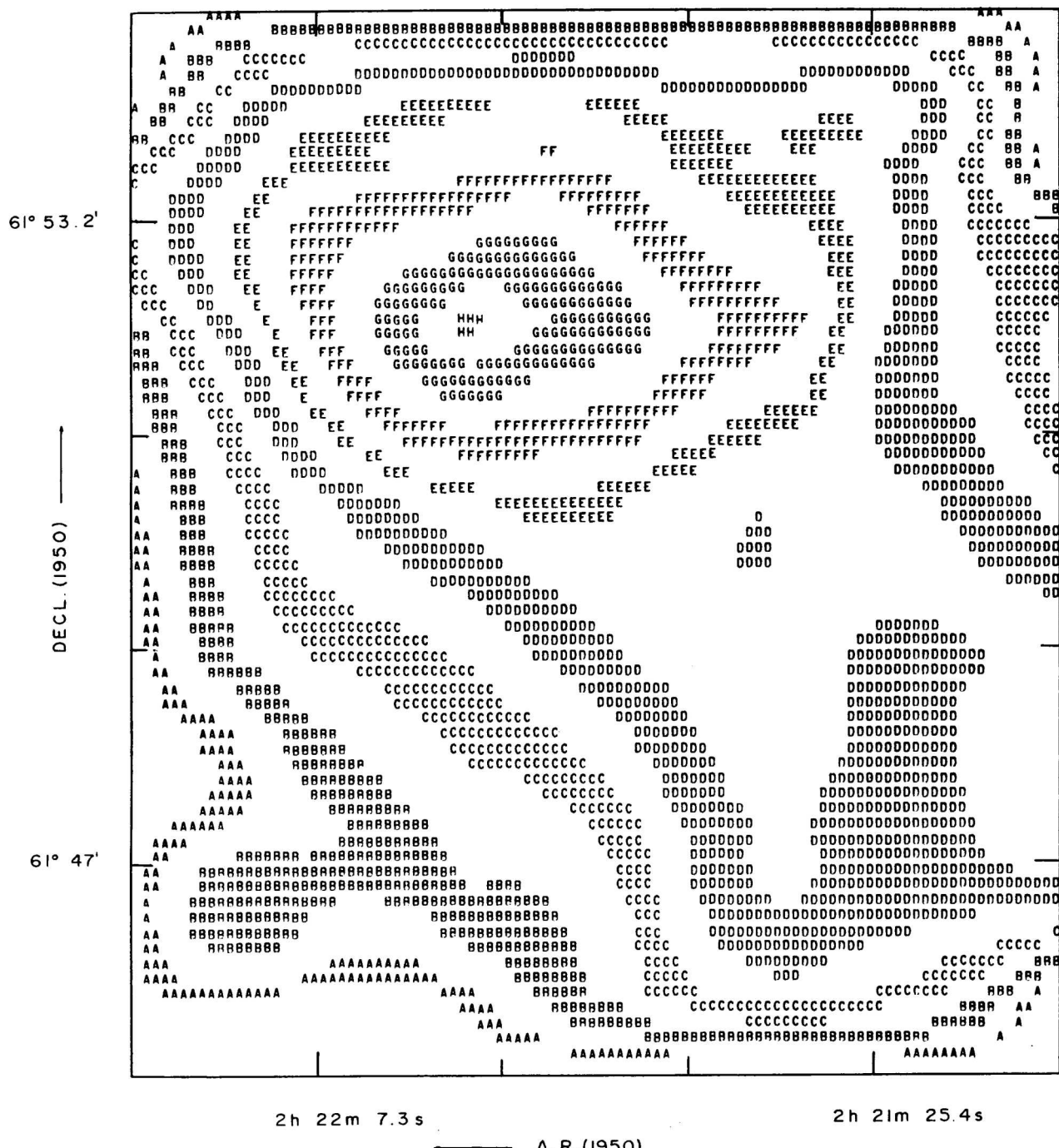


Fig. 6.—Optical depth contours of NGC 896. Each symbol represents the following range of optical depth values: $1.040 \leq A \leq 1.303$, $1.828 \leq B \leq 2.354$, $2.879 \leq C \leq 3.405$, $3.930 \leq D \leq 4.456$, $4.981 \leq E \leq 5.244$, $5.770 \leq F \leq 6.295$, $6.821 \leq G \leq 7.346$, $7.604 = H$.

62° 2.0'
DEC'L. (1950) ↑
62° 1.2'

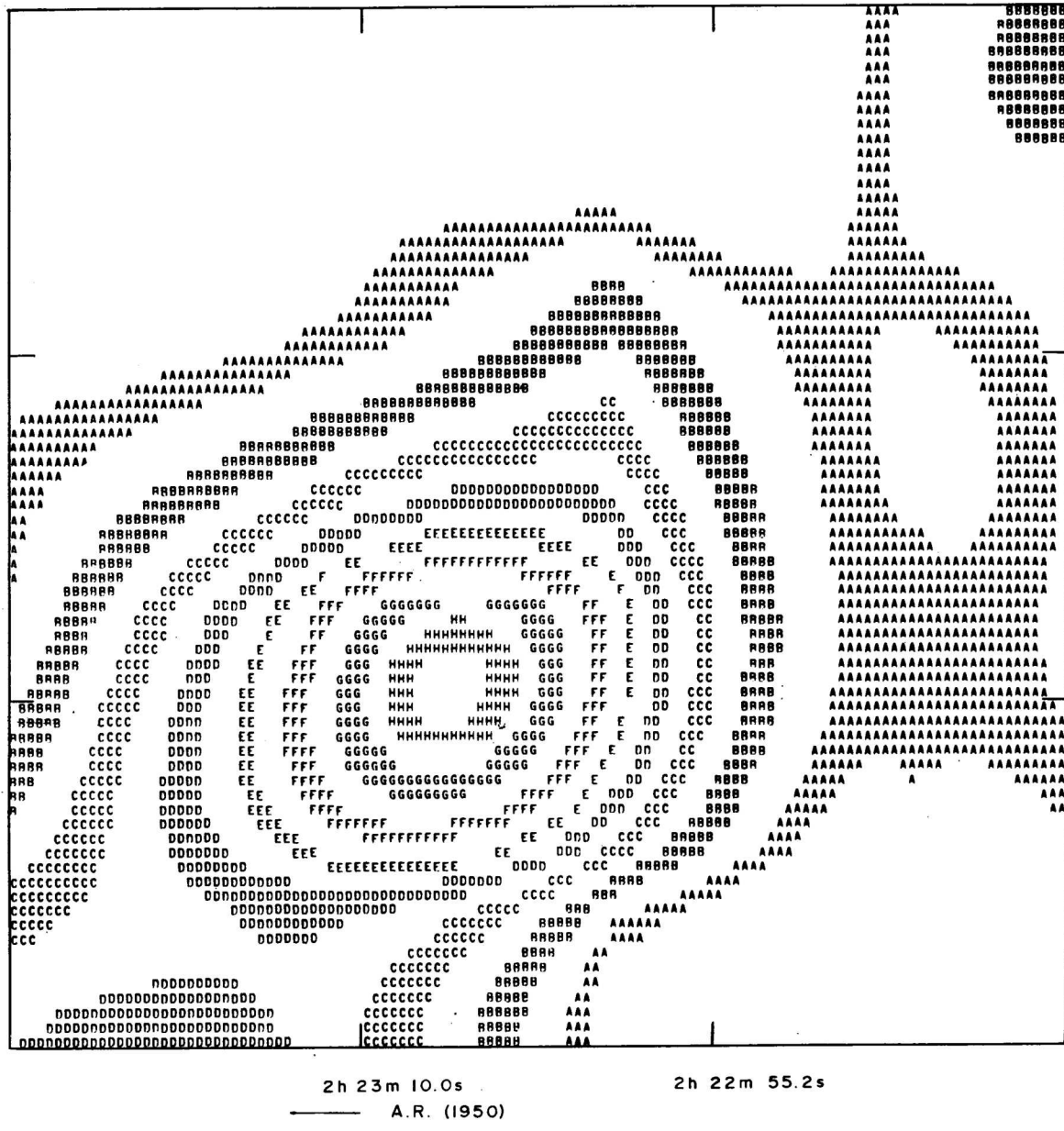


Fig. 7.—Observed intensity contours of IC 1795. Each symbol represents the following range of intensities ($10^{-4} \text{ erg cm}^{-2} \text{ sec}^{-1} \text{ sterad}^{-1}$): $0.552 \leq A \leq 0.665$, $0.890 \leq B \leq 1.115$, $1.341 \leq C \leq 1.566$, $1.791 \leq D \leq 2.016$, $2.242 \leq E \leq 2.354$, $2.579 \leq F \leq 2.805$, $3.030 \leq G \leq 3.255$, $3.368 \leq H \leq 3.480$.

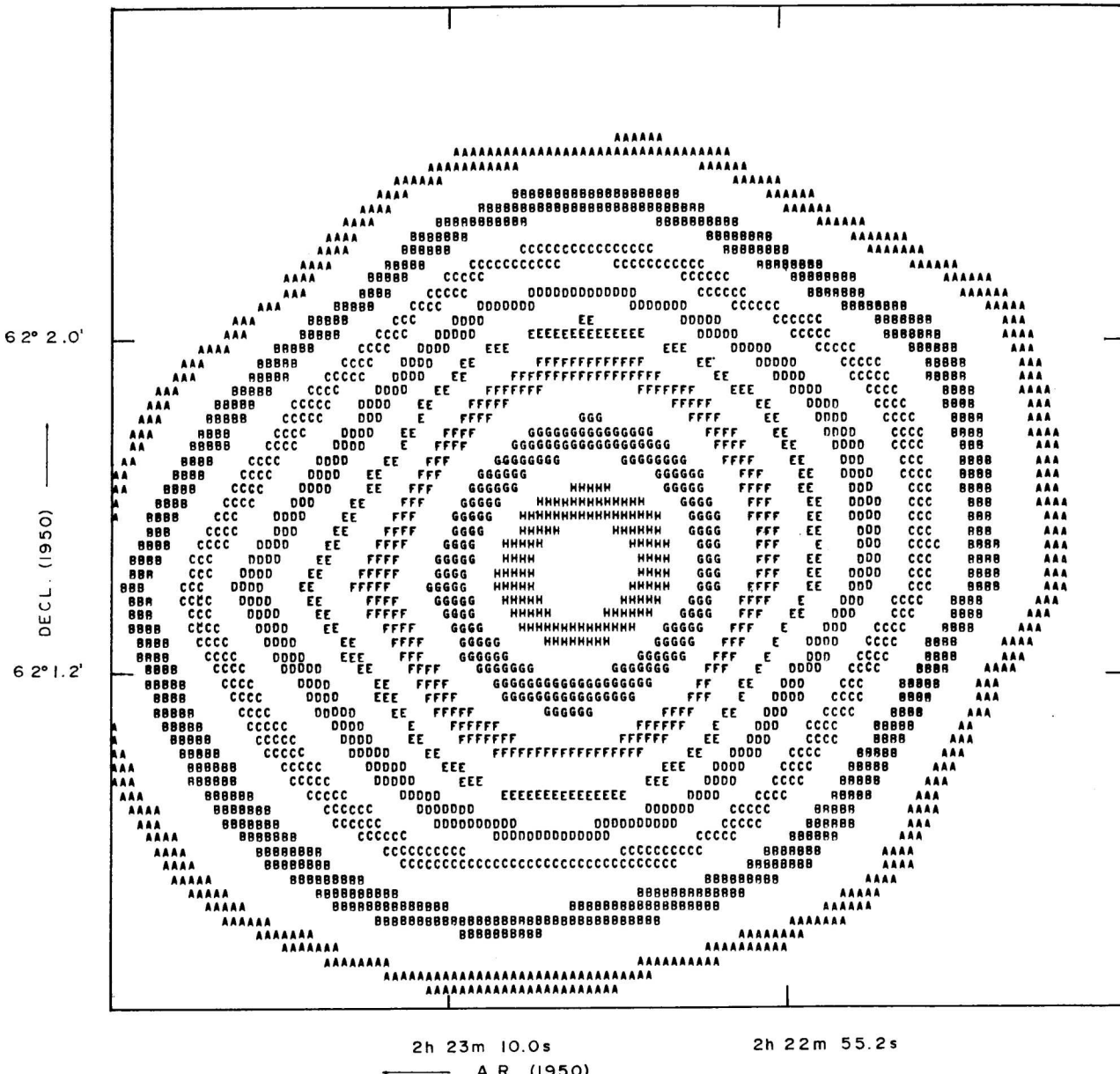


Fig. 8.—Calculated intensity contours of IC 1795. Each symbol represents the following range of intensities ($10^{-4} \text{ erg cm}^{-2} \text{ sec}^{-1} \text{ sterad}^{-1}$): $0.272 \leq A \leq 0.344$, $0.487 \leq B \leq 0.630$, $0.773 \leq C \leq 0.916$, $1.059 \leq D \leq 1.202$, $1.245 \leq E \leq 1.416$, $1.559 \leq F \leq 1.702$, $1.845 \leq G \leq 1.988$, $2.059 \leq H \leq 2.131$.

62° 2' 0"

DEC.L. (1950) ↑

62° 1' 2"



2 h 23 m 10.0 s

— A.R. (1950) —

2 h 22 m 55.2 s

Fig. 9.—Optical depth contours of IC 1795. Each symbol represents the following range of optical depth values: 0.862 $\leq A \leq 1.030$, 1.365 $\leq B \leq 1.701$, 2.036 $\leq C \leq 2.372$, 2.707 $\leq D \leq 3.043$, 3.378 $\leq E \leq 3.546$, 3.881 $\leq F \leq 4.216$, 4.552 $\leq G \leq 4.887$, 5.055 $\leq H \leq 5.223$.

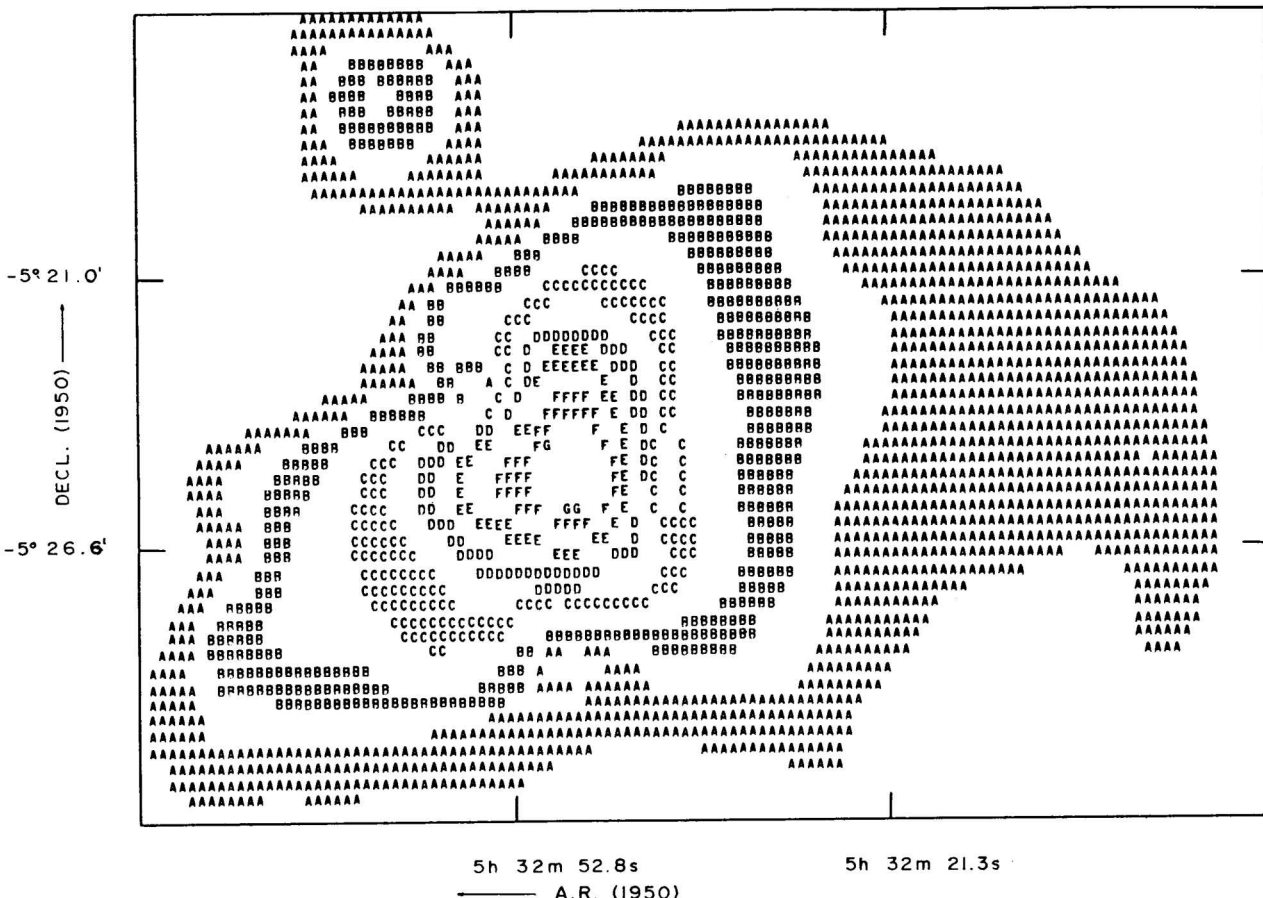


Fig. 10.—Observed intensity contours of NGC 1976 + NGC 1982. Each symbol represents the following range of intensities (10^{-2} erg cm^{-2} sec $^{-1}$ sterad $^{-1}$): $0.201 \leq A \leq 0.320$, $0.438 \leq B \leq 0.675$, $1.149 \leq C \leq 1.623$, $2.333 \leq D \leq 3.281$, $4.465 \leq E \leq 6.005$, $8.019 \leq F \leq 10.150$, $11.570 \leq G \leq 11.930$.

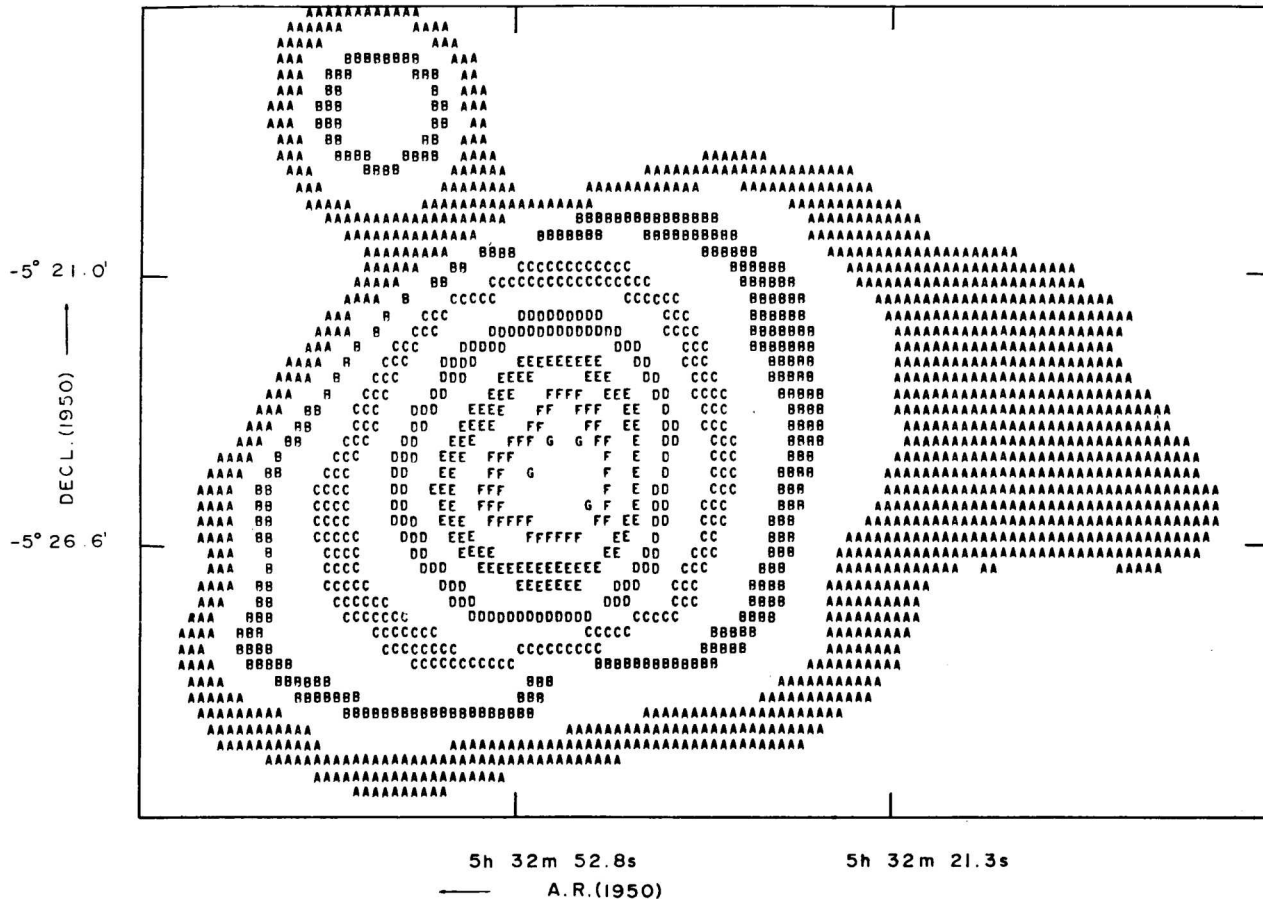


Fig. 11.—Calculated intensity contours of NGC 1976 + NGC 1982. Each symbol represents the following range of intensities (10^{-2} erg cm^{-2} sec $^{-1}$ sterad $^{-1}$): $0.838 \leq A \leq 1.241$, $1.645 \leq B \leq 2.049$, $3.261 \leq C \leq 4.877$, $7.301 \leq D \leq 10.130$, $14.170 \leq E \leq 21.040$, $28.710 \leq F \leq 35.980$, $40.830 \leq G \leq 42.040$.



Fig. 12.—Optical depth contours of NGC 1976 + NGC 1982. Each symbol represents the following range of optical depth values: $0.987 \leq A \leq 1.284$, $1.582 \leq B \leq 1.879$, $2.177 \leq C \leq 2.474$, $2.772 \leq D \leq 3.218$, $3.665 \leq E \leq 4.111$.



Fig. 13.—Observed intensity contours of NGC 2024. Each symbol represents the following range of intensities (10^{-4} erg $\text{cm}^{-2} \text{ sec}^{-1} \text{ sterad}^{-1}$): $0.698 \leq A \leq 0.797$, $0.996 \leq B \leq 1.195$, $1.394 \leq C \leq 1.593$, $1.792 \leq D \leq 1.990$, $2.189 \leq E \leq 2.388$, $2.587 \leq F \leq 2.786$, $2.985 \leq G \leq 3.184$, $3.283 \leq H \leq 3.383$.

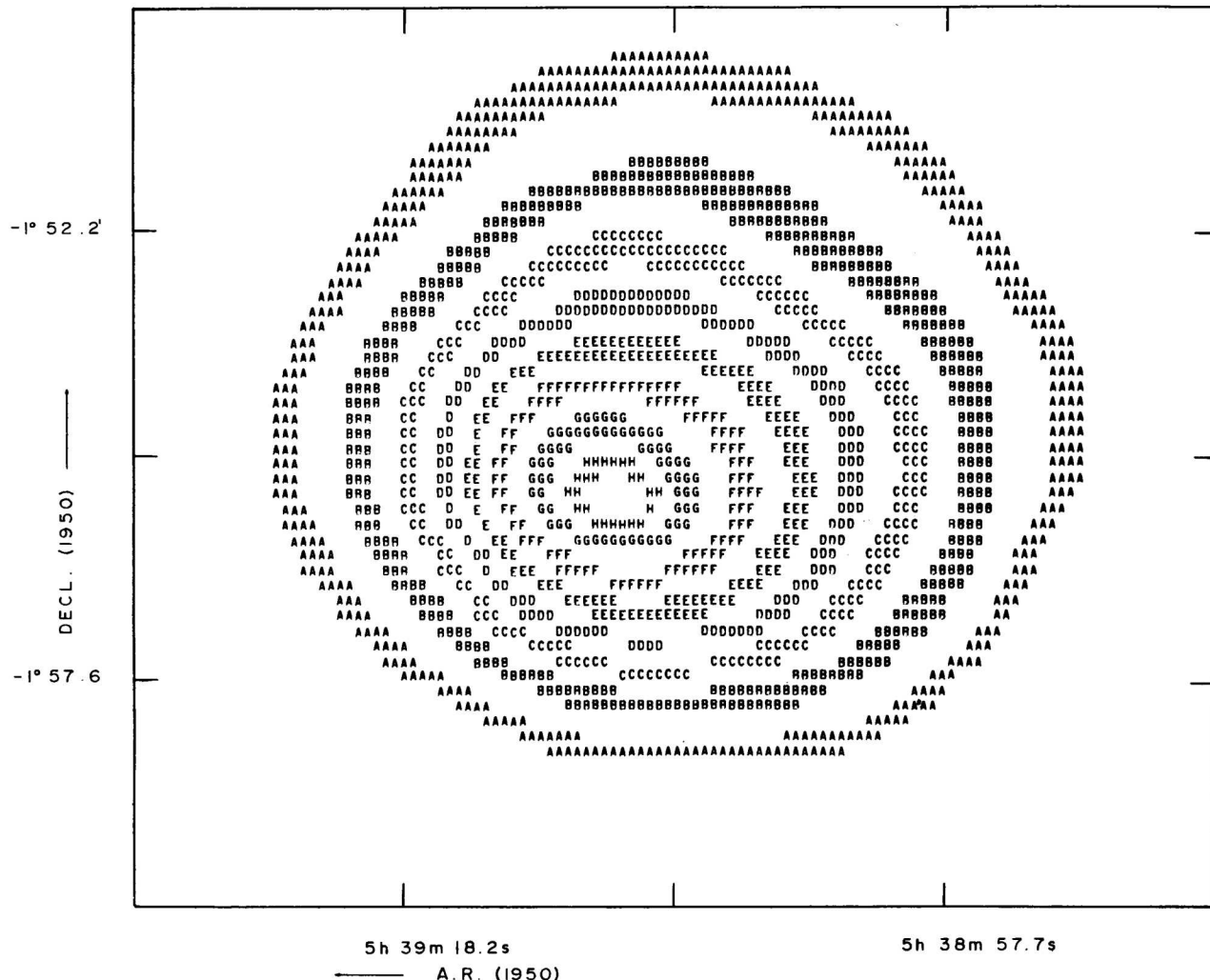


Fig. 14.—Calculated intensity contours of NGC 2024. Each symbol represents the following range of intensities (10^{-2} erg $cm^{-2} sec^{-1} sterad^{-1}$): $0.760 \leq A \leq 0.951$, $1.333 \leq B \leq 1.714$, $2.096 \leq C \leq 2.478$, $2.859 \leq D \leq 3.241$, $3.623 \leq E \leq 4.005$, $4.386 \leq F \leq 4.768$, $5.150 \leq G \leq 5.532$, $5.722 \leq H \leq 5.913$

-1° 52.2'

DEC L (1950) ↓

-1° 57.6'



5h 39m 18.2s

5h 38m 57.7s

A R (1950)

Fig. 15.—Optical depth contours of NGC 2024. Each symbol represents the following range of optical depth values: $0.864 \leq A \leq 1.087$, $1.534 \leq B \leq 1.982$, $2.429 \leq C \leq 2.876$, $3.323 \leq D \leq 3.770$, $4.218 \leq E \leq 4.441$, $4.889 \leq F \leq 5.336$, $5.783 \leq G \leq 6.007$, $6.230 \leq H \leq 6.454$.

TABLE 1

OBSERVED INTENSITY OF NGC 896
(ERGS/SQ.CM./SEC/STERAD)

DECL/R.A.*	2H	22M 21.35	22M 14.95	22M 8.65	22M 2.25	21M 55.95	21M 49.55	21M 43.25	21M 36.85
61° 55'.3	*	6.1528e-05	7.9258e-05	6.7058e-05	7.3638e-05	7.6748e-05	5.3588e-05	4.7588e-05	3.5818e-05
61 54.5	*	7.8198e-05	9.9438e-05	8.0888e-05	8.8988e-05	9.3578e-05	6.5258e-05	5.4538e-05	3.3488e-05
61 53.7	*	8.1838e-05	1.0318e-04	9.4018e-05	1.3148e-04	1.1398e-04	6.9528e-05	6.0848e-05	5.0478e-05
61 52.9	*	1.5648e-04	1.5798e-04	1.2218e-04	1.3398e-04	1.0568e-04	6.8458e-05	5.7268e-05	4.9598e-05
61 52.1	*	3.2268e-04	2.7548e-04	1.6388e-04	8.0538e-05	4.7608e-05	4.0628e-05	3.2088e-05	2.4608e-05
61 51.3	*	3.9978e-04	3.3408e-04	2.0978e-04	1.1218e-04	7.1188e-05	6.9008e-05	4.9198e-05	4.1778e-05
61 50.5	*	4.1908e-04	3.5758e-04	2.6818e-04	2.1668e-04	1.6008e-04	1.1428e-04	1.0868e-04	1.0608e-04
61 49.7	*	4.1528e-04	3.5608e-04	3.0948e-04	3.0948e-04	2.5908e-04	1.8728e-04	1.4628e-04	1.2828e-04
61 48.9	*	3.6978e-04	3.2088e-04	3.4978e-04	4.3798e-04	3.9888e-04	2.7698e-04	1.4788e-04	1.1238e-04
61 48.1	*	3.3448e-04	2.8288e-04	3.4418e-04	4.6618e-04	4.9178e-04	4.3318e-04	2.4378e-04	1.2858e-04
61 47.3	*	2.9848e-04	2.2718e-04	2.8568e-04	3.9328e-04	5.7638e-04	7.3808e-04	4.7438e-04	1.7388e-04
61 46.5	*	2.6088e-04	1.9318e-04	2.5278e-04	3.5938e-04	5.5948e-04	7.5878e-04	5.2158e-04	1.9178e-04
61 45.7	*	2.1198e-04	1.6038e-04	2.2148e-04	3.4938e-04	4.3618e-04	5.1138e-04	4.2068e-04	1.9638e-04
61 44.9	*	1.9798e-04	1.8588e-04	2.2508e-04	2.9398e-04	3.2228e-04	3.5438e-04	3.2498e-04	1.7788e-04
	*								
DECL/R.A.*	2H	21M 30.55	21M 24.15	21M 17.85	21M 11.45				
61° 55'.3	*	3.7268e-05	3.1058e-05	2.8168e-05	3.8118e-05				
61 54.5	*	2.9858e-05	1.8058e-05	2.9338e-05	4.7828e-05				
61 53.7	*	3.4048e-05	3.3728e-05	5.8858e-05	5.7478e-05				
61 52.9	*	3.0628e-05	3.4438e-05	6.1068e-05	5.3758e-05				
61 52.1	*	1.5978e-05	2.5058e-05	4.0038e-05	3.3358e-05				
61 51.3	*	2.6118e-05	2.6508e-05	3.2458e-05	2.5098e-05				
61 50.5	*	6.2308e-05	3.2658e-05	2.9018e-05	2.3268e-05				
61 49.7	*	8.2658e-05	5.1138e-05	3.6418e-05	2.5728e-05				
61 48.9	*	9.3408e-05	8.5058e-05	5.8458e-05	3.6608e-05				
61 48.1	*	1.0748e-04	1.1228e-04	7.0708e-05	3.8828e-05				
61 47.3	*	1.2478e-04	1.4668e-04	8.1318e-05	3.3498e-05				
61 46.5	*	1.3228e-04	1.4518e-04	7.6668e-05	3.2598e-05				
61 45.7	*	1.3538e-04	1.0678e-04	5.2598e-05	3.3578e-05				
61 44.9	*	1.2198e-04	7.9698e-05	4.2168e-05	3.6378e-05				

The necessity of a recalibration of the Orion Nebula was evident only after the isophotes for it were obtained. This arises from the circumstance that the analyzing beam of the microphotometer averages out densities in the central overexposed part of Orion causing an underestimation of the intensity values. This effect was not present in the other nebulae.

The recalibration was made in the following way. The H α intensity values first found (H α intensity before recalibration) were compared in a separate way with H α intensity measurements by Méndez (1967), Boyce (1966) and O'Dell and Hubbard (1965). Curve *A* in Figure 3 is the recalibration curve using Méndez values. Similarly, curves *B* and *C* are the recalibration curves resulting from the comparison with O'Dell and Hubbard and Boyce measurements. Curve *D* used in the recalibration is the average of curves *A* and *B*. Curve *C* was not taken into account because it diverges too much from the curves *A* and *B*.

The [N II]/H α ratio of intensities was assumed to be constant within each nebula with values 0.8 for Orion and 0.4 for the other nebulae. These values were obtained averaging Johnson's (1953) measurements. With this assumption, the correction for the contribution of the [N II] lines is made by using the values of H α intensities in the density-intensity curve. This correction also takes into account any contribution where the ratio of intensity with respect to H α is constant. This is approximately the case of the nebular continuum band obtained with the filter-plate combination.

TABLE 2

OPTICAL DEPTH OF NGC 896

DECL/R.A.*	2H	22M 21.3S	22M 14.9S	22M 8.6S	22M 2.2S	21M 55.9S	21M 49.5S	21M 43.2S	21M 36.4S
61° 55'.3	*	4.005e-01							
61 54.5	*	4.005e-01	2.750e+00	3.819e+00	4.171e+00	4.327e+00	4.475e+00	4.203e+00	3.950e+00
61 53.7	*	2.988e+00	4.027e+00	5.019e+00	5.110e+00	5.389e+00	5.623e+00	5.308e+00	4.880e+00
61 52.9	*	3.238e+00	4.630e+00	5.850e+00	6.319e+00	6.675e+00	6.697e+00	6.096e+00	5.464e+00
61 52.1	*	2.066e+00	3.963e+00	5.535e+00	6.916e+00	7.609e+00	7.231e+00	6.933e+00	6.209e+00
61 51.3	*	1.461e+00	3.078e+00	4.731e+00	5.978e+00	6.566e+00	6.250e+00	6.043e+00	5.338e+00
61 50.5	*	1.042e+00	2.484e+00	3.517e+00	4.272e+00	4.871e+00	5.060e+00	4.793e+00	4.396e+00
61 49.7	*	8.740e-01	2.241e+00	3.272e+00	3.602e+00	3.969e+00	4.415e+00	4.621e+00	4.352e+00
61 48.9	*	7.183e-01	1.994e+00	2.627e+00	2.948e+00	3.309e+00	3.877e+00	4.369e+00	4.481e+00
61 48.1	*	7.196e-01	1.037e+00	2.014e+00	2.447e+00	2.864e+00	3.179e+00	3.815e+00	4.404e+00
61 47.3	*	7.521e-01	1.146e+00	1.416e+00	1.977e+00	2.421e+00	2.560e+00	3.163e+00	4.144e+00
61 46.5	*	7.939e-01	1.991e+00	1.783e+00	1.639e+00	2.063e+00	2.215e+00	2.873e+00	4.014e+00
61 45.7	*	8.283e-01	9.796e-01	8.502e-01	7.079e-01	1.167e+00	1.946e+00	2.638e+00	3.407e+00
61 44.9	*	8.528e-01	9.174e-01	8.263e-01	4.005e-01	4.005e-01	4.005e-01	4.005e-01	4.005e-01

DECL/R.A.*	2H	21M 30.5S	21M 24.1S	21M 17.8S	21M 11.4S
61° 55'.3	*	4.005e-01	4.005e-01	4.005e-01	4.005e-01
61 54.5	*	4.094e+00	4.189e+00	3.030e+00	4.005e-01
61 53.7	*	4.806e+00	4.256e+00	3.026e+00	4.005e-01
61 52.9	*	5.258e+00	4.454e+00	3.307e+00	2.942e+00
61 52.1	*	5.688e+00	4.336e+00	3.535e+00	2.545e+00
61 51.3	*	4.978e+00	4.178e+00	3.737e+00	2.800e+00
61 50.5	*	4.380e+00	4.474e+00	4.090e+00	3.519e+00
61 49.7	*	4.394e+00	4.410e+00	4.367e+00	4.207e+00
61 48.9	*	4.499e+00	4.215e+00	4.278e+00	4.541e+00
61 48.1	*	4.507e+00	4.225e+00	4.396e+00	4.766e+00
61 47.3	*	4.340e+00	3.989e+00	4.291e+00	4.629e+00
61 46.5	*	4.283e+00	3.974e+00	3.921e+00	3.733e+00
61 45.7	*	3.588e+00	3.193e+00	2.501e+00	4.005e-01
61 44.9	*	4.005e-01	4.005e-01	4.005e-01	4.005e-01

TABLE 3

OBSERVED INTENSITY OF IC 1795
(ERGS/SQ.CM./SEC/STERAD)

DECL/R.A.*	2H	23M 24.8S	23M 18.4S	23M 12.1S	23M 5.7S	22M 59.4S	22M 53.0S	22M 46.7S	22M 40.3S
62° 4.9	*	1.653e-05	1.385e-05	2.889e-05	2.183e-05	1.206e-05	2.007e-05	6.802e-05	8.752e-05
62 4.1	*	2.356e-05	2.272e-05	4.215e-05	3.971e-05	3.241e-05	2.986e-05	6.980e-05	8.328e-05
62 3.3	*	3.872e-05	3.729e-05	4.630e-05	6.426e-05	9.741e-05	5.990e-05	5.056e-05	6.756e-05
62 2.5	*	5.246e-05	7.296e-05	1.047e-04	1.420e-04	1.535e-04	7.680e-05	4.677e-05	6.156e-05
62 1.7	*	6.208e-05	1.417e-04	2.466e-04	3.214e-04	2.425e-04	9.304e-05	5.652e-05	6.511e-05
62 0.9	*	8.969e-05	1.723e-04	2.722e-04	3.294e-04	2.233e-04	8.374e-05	5.226e-05	5.773e-05
62 0.1	*	1.365e-04	1.649e-04	1.843e-04	1.612e-04	7.474e-05	3.721e-05	2.980e-05	3.590e-05
61 59.3	*	1.748e-04	1.895e-04	1.696e-04	1.113e-04	3.715e-05	3.282e-05	3.617e-05	3.650e-05

TABLE 4
OPTICAL DEPTH OF IC 1795

DECL/R.A.*	2H	23M 24.8S	23M 18.4S	23M 12.1S	23M 5.7S	22M 59.4S	22M 53.0S	22M 46.7S	22M 40.3S
62° 4' 9"	*	4.005E-01							
62 4.1	*	4.005E-01	2.891E+00	3.829E+00	4.282E+00	4.481E+00	3.669E+00	1.431E+00	4.005E-01
62 3.3	*	1.847E+00	4.041E+00	4.965E+00	5.158E+00	4.583E+00	4.526E+00	4.109E+00	1.452E+00
62 2.5	*	3.618E+00	4.597E+00	4.858E+00	4.885E+00	4.736E+00	4.998E+00	4.623E+00	2.818E+00
62 1.7	*	4.174E+00	4.394E+00	4.237E+00	4.185E+00	4.397E+00	4.887E+00	4.512E+00	3.076E+00
62 0.9	*	3.493E+00	3.808E+00	3.864E+00	3.966E+00	4.205E+00	4.512E+00	3.797E+00	2.079E+00
62 0.1	*	2.276E+00	3.234E+00	3.642E+00	3.872E+00	4.464E+00	4.628E+00	3.496E+00	4.005E-01
61 59.3	*	4.005E-01	4.005E-01	1.950E+00	2.813E+00	3.286E+00	1.976E+00	4.005E-01	4.005E-01
	*								

The other nebulae were calibrated photographically by comparison with Orion. An H α extinction of 0.183 mag/atm-mass was used to correct for atmospheric extinction. It was estimated from the extinction coefficients given by Taylor (1963) for Pine Bluff, Wisconsin, interpolating for H α and correcting for the difference in altitude between Tonantzintla and Pine Bluff.

The total logarithmic probable error is estimated to be ± 0.2 with internal logarithmic probable errors of ± 0.1 .

III. Comparison between Radio and Optical Data

As explained in Paper I the observed H α intensity (I_{OBS}) was compared with the H α intensity derived from the radio observations by theoretical considerations (I_{CAL}).

The angular resolution of the optical observations was reduced to match the angular resolution of the radio data. This was done in a crude way by setting the microphotometer analyzing beam at its maximum aperture equal to 90'' in diameter (the radio HPBW is 120'').

From the comparison of I_{OBS} and I_{CAL} , the optical depth $\tau = \log_e(I_{CAL}/I_{OBS})$ can be calculated under the three following assumptions; *a*) the difference between I_{CAL} and I_{OBS} is due exclusively to interstellar extinction, *b*) the material responsible for the extinction is optically thin to free-free radiation in the radio wavelength region, *c*) this material is sufficiently far from the nebulae so that no light coming from the nebulae or from any other source is scattered into the beam towards the earth.

The optical isophotes of NGC 896, IC 1795, Orion and NGC 2024 are shown in Figures 4, 7, 10 and 13, while the corresponding I_{OBS} values are presented in Tables 1, 3, 5 and 7. The calculated H α intensity contours appear in Figures 5, 8, 11 and 14. Similarly, the optical depth contours are shown in Figures 6, 9, 12 and 15. The Tables 2, 4, 6 and 8 give the corresponding optical depth values.

TABLE 5

OBSERVED INTENSITY OF NGC 1976+NGC 1982
(ERGS/SQ.CM./SEC/STERAD)

DECL/R.A.*	5H 33m 24.4S	33m 21.1S	33m 17.8S	33m 14.6S	33m 11.3S	33m 8.1S	33m 4.8S	33m 1.5S
-5° 15'.4	* 5.412E-05	6.515E-05	1.867E-04	4.927E-04	1.149E-03	1.369E-03	1.369E-03	1.121E-03
-5 16.2	* 6.581E-05	8.123E-05	2.148E-04	5.436E-04	1.458E-03	2.300E-03	2.984E-03	2.456E-03
-5 17.0	* 8.342E-05	1.014E-04	1.650E-04	3.088E-04	1.344E-03	3.682E-03	6.240E-03	5.154E-03
-5 17.8	* 9.538E-05	1.117E-04	1.526E-04	2.498E-04	1.306E-03	3.767E-03	6.411E-03	5.354E-03
-5 18.6	* 9.957E-05	1.107E-04	1.589E-04	3.105E-04	1.293E-03	2.587E-03	3.584E-03	3.136E-03
-5 19.4	* 1.175E-04	1.188E-04	1.558E-04	2.916E-04	1.043E-03	1.734E-03	2.087E-03	1.987E-03
-5 20.2	* 1.562E-04	1.330E-04	1.348E-04	1.895E-04	4.492E-04	6.861E-04	8.966E-04	9.500E-04
-5 21.0	* 1.610E-04	1.464E-04	1.637E-04	2.211E-04	2.740E-04	2.902E-04	4.556E-04	9.966E-04
-5 21.8	* 9.695E-05	1.291E-04	2.213E-04	3.535E-04	3.893E-04	4.438E-04	7.475E-04	2.263E-03
-5 22.6	* 1.815E-04	2.280E-04	3.387E-04	5.225E-04	6.311E-04	7.788E-04	1.407E-03	3.142E-03
-5 23.4	* 4.183E-04	4.141E-04	3.972E-04	5.674E-04	8.109E-04	1.037E-03	1.909E-03	2.514E-03
-5 24.2	* 5.730E-04	6.754E-04	9.202E-04	1.302E-03	1.973E-03	2.790E-03	5.068E-03	7.213E-03
-5 25.0	* 7.160E-04	1.136E-03	2.113E-03	2.964E-03	4.350E-03	6.530E-03	1.200E-02	1.945E-02
-5 25.8	* 7.538E-04	1.228E-03	2.493E-03	3.628E-03	5.807E-03	8.390E-03	1.467E-02	2.207E-02
-5 26.6	* 6.152E-04	8.535E-04	1.938E-03	3.269E-03	6.842E-03	9.133E-03	1.434E-02	1.616E-02
-5 27.4	* 7.266E-04	1.039E-03	2.501E-03	3.928E-03	7.267E-03	9.066E-03	1.314E-02	1.381E-02
-5 28.2	* 1.087E-03	1.762E-03	4.373E-03	5.868E-03	7.184E-03	7.942E-03	1.008E-02	1.328E-02
-5 29.0	* 1.274E-03	2.098E-03	4.614E-03	5.821E-03	6.308E-03	6.605E-03	7.598E-03	1.054E-02
-5 29.8	* 1.397E-03	2.279E-03	3.473E-03	3.919E-03	4.318E-03	4.608E-03	4.968E-03	5.424E-03
-5 30.6	* 1.367E-03	2.153E-03	2.732E-03	2.810E-03	3.000E-03	3.193E-03	3.145E-03	2.754E-03
-5 31.4	* 1.142E-03	1.606E-03	1.945E-03	1.908E-03	1.948E-03	2.071E-03	1.977E-03	1.839E-03
-5 32.2	* 1.004E-03	1.317E-03	1.416E-03	1.303E-03	1.272E-03	1.348E-03	1.216E-03	1.087E-03
DECL/R.A.*	5H 32m 58.3S	32m 55.0S	32m 51.8S	32m 48.5S	32m 45.2S	32m 42.0S	32m 38.7S	32m 35.5S
-5° 15'.4	* 4.777E-04	2.855E-04	2.948E-04	3.040E-04	2.796E-04	2.454E-04	2.700E-04	2.420E-04
-5 16.2	* 1.184E-03	5.807E-04	4.294E-04	4.371E-04	4.153E-04	3.867E-04	4.282E-04	4.226E-04
-5 17.0	* 2.715E-03	1.167E-03	5.658E-04	5.365E-04	4.864E-04	4.642E-04	4.680E-04	4.948E-04
-5 17.8	* 2.995E-03	1.402E-03	7.680E-04	7.998E-04	9.049E-04	9.928E-04	1.190E-03	1.337E-03
-5 18.6	* 2.106E-03	1.267E-03	8.395E-04	8.375E-04	1.193E-03	1.621E-03	2.504E-03	3.117E-03
-5 19.4	* 1.746E-03	1.493E-03	1.634E-03	2.269E-03	3.160E-03	3.475E-03	3.885E-03	4.177E-03
-5 20.2	* 1.035E-03	1.416E-03	2.307E-03	3.728E-03	6.399E-03	6.560E-03	5.200E-03	4.808E-03
-5 21.0	* 2.374E-03	3.401E-03	5.945E-03	9.974E-03	1.109E-02	9.728E-03	6.700E-03	5.307E-03
-5 21.8	* 6.301E-03	8.278E-03	1.168E-02	1.697E-02	1.544E-02	1.318E-02	8.631E-03	5.446E-03
-5 22.6	* 7.909E-03	9.816E-03	2.049E-02	3.880E-02	2.769E-02	1.712E-02	9.688E-03	5.990E-03
-5 23.4	* 4.801E-03	2.175E-03	3.032E-02	7.900E-02	4.700E-02	2.255E-02	9.891E-03	7.006E-03
-5 24.2	* 1.307E-02	1.885E-02	4.981E-02	1.069E-01	6.904E-02	2.453E-02	1.045E-02	7.420E-03
-5 25.0	* 3.714E-02	6.963E-02	9.068E-02	1.399E-01	1.080E-01	2.341E-02	1.119E-02	7.286E-03
-5 25.8	* 4.025E-02	7.529E-02	8.959E-02	1.280E-01	1.019E-01	2.257E-02	1.174E-02	7.423E-03
-5 26.6	* 2.420E-02	3.975E-02	4.652E-02	6.411E-02	4.729E-02	2.277E-02	1.289E-02	8.031E-03
-5 27.4	* 1.734E-02	2.385E-02	2.487E-02	3.096E-02	2.146E-02	1.790E-02	1.136E-02	7.349E-03
-5 28.2	* 1.490E-02	1.614E-02	1.180E-02	1.220E-02	1.018E-02	8.240E-03	6.747E-03	5.334E-03
-5 29.0	* 1.070E-02	9.217E-03	3.820E-03	1.336E-03	2.480E-03	3.612E-03	4.171E-03	3.944E-03
-5 29.8	* 5.240E-03	4.886E-03	3.612E-03	3.054E-03	2.702E-03	2.609E-03	2.678E-03	2.726E-03
-5 30.6	* 2.366E-03	2.121E-03	2.150E-03	1.939E-03	1.584E-03	1.487E-03	1.602E-03	1.835E-03
-5 31.4	* 1.746E-03	1.675E-03	1.516E-03	1.379E-03	1.285E-03	1.241E-03	1.217E-03	1.260E-03
-5 32.2	* 1.091E-03	1.070E-03	1.023E-03	9.872E-04	9.936E-04	9.744E-04	9.039E-04	8.999E-04

TABLE 5

OBSERVED INTENSITY OF NGC 1976+NGC 1982 (CONTINUATION)
(ERGS/SQ.CM./SEC/STERAD)

DECL/R.A.*	5H 32M 32.2S	32M 28.9S	32M 25.7S	32M 22.4S	32M 19.2S	32M 15.9S	32M 12.6S	32M 9.4S
-5° 15'.4	* 2.4888e-04	2.7098e-04	2.6620e-04	2.6858e-04	2.6650e-04	2.4148e-04	2.2328e-04	2.3488e-04
-5 16.2	* 4.5528e-04	4.9588e-04	4.9358e-04	4.9018e-04	4.7508e-04	4.4088e-04	4.2068e-04	4.1378e-04
-5 17.0	* 6.3048e-04	7.6298e-04	8.2828e-04	8.3448e-04	8.0518e-04	7.7388e-04	7.6568e-04	7.1418e-04
-5 17.8	* 1.3728e-03	1.3418e-03	1.2558e-03	1.1888e-03	1.1058e-03	1.0608e-03	1.0518e-03	9.5358e-04
-5 18.6	* 2.8598e-03	2.3758e-03	1.8758e-03	1.6178e-03	1.4138e-03	1.3358e-03	1.3308e-03	1.1568e-03
-5 19.4	* 3.6638e-03	2.9218e-03	2.2328e-03	1.9238e-03	1.7018e-03	1.6138e-03	1.5578e-03	1.3928e-03
-5 20.2	* 3.9968e-03	3.0468e-03	2.3278e-03	2.1118e-03	1.9978e-03	1.9158e-03	1.7168e-03	1.6518e-03
-5 21.0	* 4.2978e-03	3.3868e-03	2.6068e-03	2.3558e-03	2.1998e-03	2.1228e-03	1.9318e-03	1.9148e-03
-5 21.8	* 4.3898e-03	3.8848e-03	3.0798e-03	2.6788e-03	2.3498e-03	2.2988e-03	2.3008e-03	2.2918e-03
-5 22.6	* 4.6518e-03	4.1718e-03	3.2588e-03	2.8068e-03	2.3548e-03	2.2608e-03	2.2458e-03	2.2848e-03
-5 23.4	* 5.1138e-03	4.3648e-03	3.2158e-03	2.7908e-03	2.2008e-03	1.9688e-03	1.7028e-03	1.8384e-03
-5 24.2	* 5.2598e-03	4.2938e-03	3.0988e-03	2.6658e-03	2.0458e-03	1.7918e-03	1.5548e-03	1.7094e-03
-5 25.0	* 5.1158e-03	3.8628e-03	2.8228e-03	2.3778e-03	1.8208e-03	1.6418e-03	1.7158e-03	1.8254e-03
-5 25.8	* 5.0768e-03	3.6908e-03	2.6348e-03	2.1448e-03	1.6958e-03	1.5618e-03	1.7018e-03	1.7708e-03
-5 26.6	* 5.2028e-03	3.7438e-03	2.4778e-03	1.8818e-03	1.6638e-03	1.5918e-03	1.6298e-03	1.6464e-03
-5 27.4	* 4.8198e-03	3.5568e-03	2.3738e-03	1.7698e-03	1.5878e-03	1.5028e-03	1.4408e-03	1.4004e-03
-5 28.2	* 3.9158e-03	3.1888e-03	2.3808e-03	1.8638e-03	1.5088e-03	1.3098e-03	1.0508e-03	9.3168e-04
-5 29.0	* 3.2228e-03	2.8218e-03	2.2098e-03	1.7228e-03	1.3698e-03	1.1748e-03	9.0188e-04	7.6218e-04
-5 29.8	* 2.5968e-03	2.4158e-03	1.8688e-03	1.3428e-03	1.1258e-03	1.0448e-03	9.4338e-04	8.3818e-04
-5 30.6	* 1.9838e-03	1.9778e-03	1.6168e-03	1.1888e-03	1.0448e-03	1.0058e-03	9.7438e-04	8.8844e-04
-5 31.4	* 1.3198e-03	1.4548e-03	1.4298e-03	1.2628e-03	1.1658e-03	1.1218e-03	1.0998e-03	1.0278e-03
-5 32.2	* 9.5318e-04	1.0928e-03	1.1638e-03	1.0918e-03	1.0368e-03	1.0068e-03	1.0328e-03	9.9378e-04
*								
DECL/R.A.*	5H 32M 6.1S	32M 2.9S	31M 59.6S	31M 56.3S	31M 53.1S	31M 49.8S		
-5° 15'.4	* 2.8678e-04	2.9458e-04	2.9088e-04	2.7638e-04	2.9858e-04	2.8338e-04		
-5 16.2	* 4.1498e-04	4.0008e-04	3.7098e-04	3.3398e-04	3.4038e-04	3.3658e-04		
-5 17.0	* 5.6738e-04	4.9208e-04	3.9578e-04	3.1258e-04	2.6118e-04	3.0358e-04		
-5 17.8	* 6.9708e-04	5.8128e-04	4.5668e-04	3.5598e-04	2.8018e-04	3.1478e-04		
-5 18.6	* 7.7448e-04	6.4258e-04	5.2308e-04	4.3918e-04	3.7278e-04	3.4768e-04		
-5 19.4	* 9.8548e-04	7.8258e-04	6.4618e-04	5.3468e-04	4.3428e-04	3.7668e-04		
-5 20.2	* 1.3178e-03	9.4958e-04	7.7928e-04	6.2098e-04	4.7088e-04	3.9798e-04		
-5 21.0	* 1.6448e-03	1.2788e-03	1.0888e-03	8.2588e-04	5.5818e-04	4.5488e-04		
-5 21.8	* 2.0668e-03	1.8498e-03	1.6328e-03	1.1638e-03	7.1308e-04	5.5808e-04		
-5 22.6	* 2.2408e-03	2.1478e-03	1.9728e-03	1.4418e-03	7.8108e-04	6.1388e-04		
-5 23.4	* 2.2118e-03	2.2788e-03	2.1758e-03	1.7228e-03	7.3208e-04	5.9978e-04		
-5 24.2	* 2.1068e-03	2.2608e-03	2.3668e-03	1.9108e-03	8.6038e-04	7.1648e-04		
-5 25.0	* 1.8578e-03	2.0448e-03	2.6138e-03	2.0498e-03	1.1808e-03	9.8968e-04		
-5 25.8	* 1.6548e-03	1.8398e-03	2.4748e-03	2.0288e-03	1.3328e-03	1.1098e-03		
-5 26.6	* 1.4738e-03	1.5958e-03	1.8588e-03	1.8118e-03	1.4168e-03	1.1548e-03		
-5 27.4	* 1.2388e-03	1.3408e-03	1.6308e-03	1.6708e-03	1.3258e-03	1.0628e-03		
-5 28.2	* 9.0368e-04	1.0348e-03	1.7638e-03	1.5978e-03	9.8628e-04	7.5458e-04		
-5 29.0	* 7.5258e-04	8.3858e-04	1.5238e-03	1.3578e-03	8.4078e-04	6.5498e-04		
-5 29.8	* 7.5798e-04	7.1828e-04	9.1038e-04	9.1068e-04	8.4878e-04	7.2688e-04		
-5 30.6	* 7.6188e-04	6.7328e-04	6.5428e-04	6.7688e-04	7.5438e-04	6.7818e-04		
-5 31.4	* 8.2618e-04	7.5198e-04	6.7718e-04	6.1428e-04	5.9288e-04	5.5368e-04		
-5 32.2	* 8.2028e-04	7.2948e-04	6.1198e-04	4.9708e-04	4.5598e-04	4.8118e-04		
*								

TABLE 6

OPTICAL DEPTH OF NGC 1976+NGC 1982

DECL/R.A.*	5H 33M 24.4S	33M 21.1S	33M 17.8S	33M 14.6S	33M 11.3S	33M 8.1S	33M 4.8S	33M 1.5S
-5° 15'.4 *	1.955E+00	2.443E+00	2.196E+00	1.951E+00	1.663E+00	1.701E+00	1.795E+00	1.801E+00
-5 16.2 *	1.621E+00	2.516E+00	2.464E+00	2.259E+00	1.849E+00	1.726E+00	1.646E+00	1.695E+00
-5 17.0 *	2.237E+00	2.636E+00	2.693E+00	2.777E+00	2.025E+00	1.550E+00	1.322E+00	1.363E+00
-5 17.8 *	1.617E+00	2.406E+00	2.784E+00	3.060E+00	2.076E+00	1.570E+00	1.314E+00	1.345E+00
-5 18.6 *	1.486E+00	2.145E+00	2.139E+00	2.638E+00	1.906E+00	1.683E+00	1.534E+00	1.563E+00
-5 19.4 *	1.581E+00	2.135E+00	2.378E+00	2.229E+00	1.611E+00	1.701E+00	1.614E+00	1.658E+00
-5 20.2 *	1.653E+00	2.131E+00	2.481E+00	2.510E+00	2.104E+00	2.051E+00	2.130E+00	2.225E+00
-5 21.0 *	1.847E+00	2.176E+00	2.442E+00	2.535E+00	2.681E+00	2.918E+00	2.846E+00	2.481E+00
-5 21.8 *	2.734E+00	2.869E+00	2.658E+00	2.396E+00	2.548E+00	2.856E+00	2.931E+00	2.542E+00
-5 22.6 *	2.464E+00	2.349E+00	2.215E+00	2.196E+00	2.402E+00	2.785E+00	2.908E+00	2.695E+00
-5 23.4 *	1.916E+00	1.963E+00	2.163E+00	2.309E+00	2.591E+00	2.906E+00	3.016E+00	3.215E+00
-5 24.2 *	1.436E+00	1.451E+00	1.618E+00	1.907E+00	2.109E+00	2.311E+00	2.267E+00	2.424E+00
-5 25.0 *	1.398E+00	1.272E+00	1.258E+00	1.480E+00	1.666E+00	1.725E+00	1.602E+00	1.666E+00
-5 25.8 *	1.477E+00	1.441E+00	1.288E+00	1.443E+00	1.514E+00	1.560E+00	1.440E+00	1.524E+00
-5 26.6 *	1.615E+00	1.676E+00	1.425E+00	1.465E+00	1.321E+00	1.387E+00	1.323E+00	1.559E+00
-5 27.4 *	1.542E+00	1.533E+00	1.234E+00	1.334E+00	1.227E+00	1.306E+00	1.283E+00	1.449E+00
-5 28.2 *	1.359E+00	1.289E+00	9.941E-01	1.083E+00	1.149E+00	1.220E+00	1.197E+00	1.216E+00
-5 29.0 *	1.234E+00	1.122E+00	9.221E-01	9.828E-01	1.104E+00	1.190E+00	1.201E+00	1.089E+00
-5 29.8 *	9.472E-01	8.848E-01	8.439E-01	8.921E-01	1.083E+00	1.199E+00	1.239E+00	1.222E+00
-5 30.6 *	9.733E-01	8.877E-01	8.884E-01	9.413E-01	1.084E+00	1.230E+00	1.353E+00	1.432E+00
-5 31.4 *	1.109E+00	1.039E+00	1.013E+00	1.062E+00	1.097E+00	1.211E+00	1.380E+00	1.485E+00
-5 32.2 *	8.275E-01	8.237E-01	8.406E-01	8.771E-01	9.659E-01	1.045E+00	1.253E+00	1.299E+00
DECL/R.A.*	5H 32M 58.3S	32M 55.0S	32M 51.8S	32M 48.5S	32M 45.2S	32M 42.0S	32M 38.7S	32M 35.5S
-5° 15'.4 *	2.105E+00	2.067E+00	1.585E+00	1.081E+00	9.590E-01	8.435E-01	7.808E-01	7.734E-01
-5 16.2 *	1.915E+00	2.013E+00	1.837E+00	1.407E+00	1.126E+00	9.704E-01	8.450E-01	8.311E-01
-5 17.0 *	1.465E+00	1.493E+00	1.597E+00	1.309E+00	1.033E+00	9.728E-01	9.567E-01	8.617E-01
-5 17.8 *	1.414E+00	1.456E+00	1.372E+00	9.369E-01	8.161E-01	7.679E-01	8.044E-01	9.195E-01
-5 18.6 *	1.598E+00	1.673E+00	1.640E+00	1.451E+00	1.345E+00	1.183E+00	1.054E+00	9.969E-01
-5 19.4 *	1.648E+00	1.721E+00	1.671E+00	1.441E+00	1.253E+00	1.223E+00	1.167E+00	1.097E+00
-5 20.2 *	2.252E+00	2.147E+00	1.939E+00	1.646E+00	1.243E+00	1.159E+00	1.230E+00	1.187E+00
-5 21.0 *	2.103E+00	2.224E+00	1.892E+00	1.515E+00	1.276E+00	1.187E+00	1.283E+00	1.319E+00
-5 21.8 *	2.019E+00	2.014E+00	1.854E+00	1.563E+00	1.485E+00	1.359E+00	1.354E+00	1.411E+00
-5 22.6 *	2.233E+00	2.351E+00	1.909E+00	1.435E+00	1.437E+00	1.454E+00	1.515E+00	1.398E+00
-5 23.4 *	3.039E+00	4.247E+00	2.102E+00	1.382E+00	1.434E+00	1.576E+00	1.654E+00	1.497E+00
-5 24.2 *	2.402E+00	2.448E+00	1.867E+00	1.331E+00	1.426E+00	1.707E+00	1.779E+00	1.560E+00
-5 25.0 *	1.605E+00	1.500E+00	1.514E+00	1.240E+00	1.167E+00	1.720E+00	1.707E+00	1.595E+00
-5 25.8 *	1.474E+00	1.389E+00	1.428E+00	1.200E+00	1.137E+00	1.672E+00	1.630E+00	1.519E+00
-5 26.6 *	1.677E+00	1.620E+00	1.666E+00	1.404E+00	1.338E+00	1.446E+00	1.396E+00	1.281E+00
-5 27.4 *	1.558E+00	1.656E+00	1.779E+00	1.579E+00	1.551E+00	1.344E+00	1.212E+00	1.198E+00
-5 28.2 *	1.352E+00	1.487E+00	1.763E+00	1.652E+00	1.548E+00	1.364E+00	1.280E+00	1.235E+00
-5 29.0 *	1.157E+00	1.325E+00	1.944E+00	2.717E+00	2.005E+00	1.546E+00	1.343E+00	1.279E+00
-5 29.8 *	1.295E+00	1.387E+00	1.560E+00	1.563E+00	1.541E+00	1.487E+00	1.404E+00	1.342E+00
-5 30.6 *	1.449E+00	1.516E+00	1.497E+00	1.547E+00	1.634E+00	1.617E+00	1.497E+00	1.335E+00
-5 31.4 *	1.371E+00	1.356E+00	1.388E+00	1.424E+00	1.444E+00	1.426E+00	1.405E+00	1.368E+00
-5 32.2 *	1.197E+00	1.169E+00	1.221E+00	1.353E+00	1.376E+00	1.368E+00	1.465E+00	1.545E+00

TABLE 6

OPTICAL DEPTH OF NGC 1976+NGC 1982 (CONTINUATION)

DECL/R.A.*	5H	32° 32.2S	32° 28.9S	32° 25.7S	32° 22.4S	32° 19.2S	32° 15.9S	32° 12.6S	32° 9.4S
-5° 15'.4	*	7.935E-01	7.961E-01	7.803E-01	7.567E-01	7.860E-01	7.450E-01	7.618E-01	7.376E-01
-5 16.2	*	8.196E-01	7.828E-01	7.846E-01	7.695E-01	7.520E-01	7.699E-01	7.488E-01	7.697E-01
-5 17.0	*	7.760E-01	7.641E-01	7.453E-01	7.486E-01	7.540E-01	7.403E-01	7.231E-01	7.397E-01
-5 17.8	*	8.979E-01	7.531E-01	8.009E-01	8.539E-01	8.586E-01	8.345E-01	8.342E-01	8.899E-01
-5 18.6	*	1.015E+00	1.051E+00	1.120E+00	1.191E+00	1.267E+00	1.276E+00	1.263E+00	1.320E+00
-5 19.4	*	1.135E+00	1.227E+00	1.330E+00	1.296E+00	1.262E+00	1.220E+00	1.192E+00	1.208E+00
-5 20.2	*	1.202E+00	1.270E+00	1.333E+00	1.295E+00	1.223E+00	1.183E+00	1.228E+00	1.224E+00
-5 21.0	*	1.358E+00	1.403E+00	1.445E+00	1.402E+00	1.379E+00	1.366E+00	1.395E+00	1.362E+00
-5 21.8	*	1.398E+00	1.353E+00	1.398E+00	1.390E+00	1.386E+00	1.341E+00	1.306E+00	1.270E+00
-5 22.6	*	1.375E+00	1.324E+00	1.361E+00	1.374E+00	1.355E+00	1.251E+00	1.181E+00	1.143E+00
-5 23.4	*	1.387E+00	1.318E+00	1.385E+00	1.381E+00	1.416E+00	1.423E+00	1.467E+00	1.334E+00
-5 24.2	*	1.455E+00	1.352E+00	1.466E+00	1.449E+00	1.549E+00	1.534E+00	1.563E+00	1.440E+00
-5 25.0	*	1.458E+00	1.395E+00	1.463E+00	1.503E+00	1.651E+00	1.675E+00	1.620E+00	1.553E+00
-5 25.8	*	1.392E+00	1.370E+00	1.471E+00	1.544E+00	1.587E+00	1.636E+00	1.638E+00	1.657E+00
-5 26.6	*	1.308E+00	1.286E+00	1.422E+00	1.500E+00	1.498E+00	1.449E+00	1.436E+00	1.438E+00
-5 27.4	*	1.255E+00	1.302E+00	1.390E+00	1.481E+00	1.423E+00	1.396E+00	1.422E+00	1.338E+00
-5 28.2	*	1.327E+00	1.340E+00	1.389E+00	1.426E+00	1.450E+00	1.438E+00	1.552E+00	1.579E+00
-5 29.0	*	1.314E+00	1.320E+00	1.405E+00	1.439E+00	1.387E+00	1.411E+00	1.558E+00	1.575E+00
-5 29.8	*	1.315E+00	1.278E+00	1.356E+00	1.469E+00	1.467E+00	1.414E+00	1.386E+00	1.367E+00
-5 30.6	*	1.233E+00	1.174E+00	1.205E+00	1.304E+00	1.330E+00	1.165E+00	1.072E+00	1.001E+00
-5 31.4	*	1.284E+00	1.204E+00	1.107E+00	1.050E+00	8.458E-01	8.057E-01	7.939E-01	7.985E-01
-5 32.2	*	1.505E+00	1.324E+00	1.138E+00	1.007E+00	9.610E-01	9.151E-01	8.929E-01	8.910E-01

DECL/R.A.*	5H	32° 6.1S	32° 2.9S	31° 59.6S	31° 56.3S	31° 53.1S	31° 49.8S
-5° 15'.4	*	7.169E-01	7.343E-01	7.349E-01	7.190E-01	7.118E-01	7.229E-01
-5 16.2	*	7.424E-01	7.478E-01	7.410E-01	7.126E-01	7.279E-01	6.972E-01
-5 17.0	*	7.781E-01	8.125E-01	8.770E-01	8.204E-01	8.009E-01	7.169E-01
-5 17.8	*	8.942E-01	9.753E-01	1.039E+00	8.696E-01	8.153E-01	7.499E-01
-5 18.6	*	1.451E+00	1.488E+00	1.468E+00	1.293E+00	1.229E+00	1.139E+00
-5 19.4	*	1.321E+00	1.290E+00	1.180E+00	1.118E+00	1.058E+00	9.907E-01
-5 20.2	*	1.315E+00	1.447E+00	1.446E+00	1.396E+00	1.389E+00	1.001E+00
-5 21.0	*	1.413E+00	1.529E+00	1.587E+00	1.653E+00	1.811E+00	1.812E+00
-5 21.8	*	1.263E+00	1.296E+00	1.321E+00	1.431E+00	1.687E+00	1.824E+00
-5 22.6	*	1.093E+00	1.093E+00	1.102E+00	1.250E+00	1.616E+00	1.666E+00
-5 23.4	*	1.182E+00	1.121E+00	1.089E+00	1.129E+00	1.570E+00	1.670E+00
-5 24.2	*	1.271E+00	1.191E+00	1.135E+00	1.165E+00	1.529E+00	1.487E+00
-5 25.0	*	1.508E+00	1.421E+00	1.202E+00	1.262E+00	1.482E+00	1.448E+00
-5 25.8	*	1.687E+00	1.586E+00	1.323E+00	1.376E+00	1.530E+00	1.405E+00
-5 26.6	*	1.470E+00	1.513E+00	1.422E+00	1.320E+00	1.321E+00	1.142E+00
-5 27.4	*	1.496E+00	1.402E+00	1.233E+00	1.164E+00	1.160E+00	9.801E-01
-5 28.2	*	1.415E+00	1.232E+00	1.012E+00	1.170E+00	1.302E+00	1.197E+00
-5 29.0	*	1.406E+00	1.263E+00	1.038E+00	1.214E+00	1.389E+00	1.295E+00
-5 29.8	*	1.347E+00	1.218E+00	1.023E+00	1.058E+00	1.022E+00	1.027E+00
-5 30.6	*	9.129E-01	9.272E-01	8.931E-01	8.890E-01	7.842E-01	7.350E-01
-5 31.4	*	8.145E-01	8.124E-01	7.979E-01	8.146E-01	7.812E-01	7.693E-01
-5 32.2	*	8.343E-01	8.411E-01	8.538E-01	8.702E-01	8.446E-01	8.118E-01

TABLE 7

OBSERVED INTENSITY OF NGC 2024
(ERGS/SQ.CM./SEC/STERAD)

DECL/R.A.*	5H 39M 28.5S	39M 25.4S	39M 22.2S	39M 19.0S	39M 15.9S	39M 12.7S	39M 9.6S	39M 6.4S
-1° 51' 0"	1.092E-04	1.225E-04	1.233E-04	1.098E-04	9.402E-05	9.557E-05	1.226E-04	1.551E-04
-1 51.8	1.076E-04	1.187E-04	1.198E-04	1.131E-04	1.111E-04	1.208E-04	1.434E-04	1.693E-04
-1 52.6	7.092E-05	7.268E-05	7.446E-05	8.759E-05	1.248E-04	1.664E-04	1.778E-04	2.208E-04
-1 53.4	6.707E-05	7.003E-05	8.929E-05	1.312E-04	1.786E-04	1.846E-04	1.836E-04	2.098E-04
-1 54.2	8.842E-05	1.073E-04	1.714E-04	2.681E-04	3.060E-04	1.827E-04	1.618E-04	1.378E-04
-1 55.0	1.026E-04	1.150E-04	1.857E-04	2.876E-04	3.065E-04	1.741E-04	1.494E-04	9.782E-05
-1 55.8	1.206E-04	9.531E-05	1.434E-04	2.069E-04	1.807E-04	1.512E-04	1.392E-04	6.893E-05
-1 56.6	1.232E-04	1.070E-04	1.270E-04	1.570E-04	1.263E-04	1.356E-04	1.281E-04	5.616E-05
-1 57.4	1.114E-04	1.560E-04	1.192E-04	9.169E-05	9.322E-05	1.105E-04	1.138E-04	6.590E-05
-1 58.2	9.955E-05	1.558E-04	1.181E-04	9.542E-05	1.179E-04	1.329E-04	1.100E-04	6.331E-05
-1 59.0	8.298E-05	1.111E-04	1.333E-04	1.898E-04	2.400E-04	2.291E-04	1.221E-04	5.209E-05
-1 59.8	6.884E-05	8.721E-05	1.223E-04	1.895E-04	2.383E-04	2.196E-04	1.107E-04	4.988E-05
DECL/R.A.*	5H 39M 3.3S	39M 0.1S	38M 57.0S	38M 53.9S	38M 50.7S	38M 47.5S		
-1° 51' 0"	1.673E-04	1.583E-04	1.180E-04	8.781E-05	6.517E-05	5.679E-05		
-1 51.8	1.502E-04	1.526E-04	1.178E-04	7.796E-05	5.955E-05	5.704E-05		
-1 52.6	1.378E-04	1.212E-04	9.665E-05	5.023E-05	4.749E-05	5.060E-05		
-1 53.4	1.177E-04	9.925E-05	8.952E-05	5.858E-05	6.525E-05	6.994E-05		
-1 54.2	8.664E-05	7.672E-05	8.934E-05	1.000E-04	1.127E-04	1.141E-04		
-1 55.0	7.167E-05	6.554E-05	9.402E-05	1.345E-04	1.542E-04	1.551E-04		
-1 55.8	7.214E-05	6.566E-05	9.083E-05	1.678E-04	1.995E-04	1.972E-04		
-1 56.6	6.400E-05	6.534E-05	1.413E-04	2.125E-04	2.385E-04	2.487E-04		
-1 57.4	4.893E-05	6.665E-05	2.748E-04	2.815E-04	2.838E-04	3.419E-04		
-1 58.2	4.312E-05	7.171E-05	2.925E-04	3.026E-04	2.867E-04	3.183E-04		
-1 59.0	4.386E-05	8.330E-05	2.077E-04	2.932E-04	2.535E-04	1.672E-04		
-1 59.8	4.770E-05	8.628E-05	1.566E-04	2.444E-04	2.036E-04	9.693E-05		

TABLE 8

OPTICAL DEPTH OF NGC 2024

DECL/R.A.*	5H	39M 28.5S	39M 25.4S	39M 22.2S	39M 19.0S	39M 15.9S	39M 12.7S	39M 9.6S	39M 6.4S
-1° 51'.0	*	4.005E-01	4.005E-01	4.005E-01	2.189E+00	3.528E+00	3.924E+00	3.802E+00	3.538E+00
-1 51.8	*	8.926E-01	1.167E+00	2.461E+00	3.526E+00	4.036E+00	4.133E+00	4.043E+00	3.869E+00
-1 52.6	*	1.981E+00	3.176E+00	3.873E+00	4.235E+00	4.227E+00	4.216E+00	4.301E+00	4.074E+00
-1 53.4	*	2.208E+00	3.513E+00	4.032E+00	4.202E+00	4.351E+00	4.709E+00	4.828E+00	4.583E+00
-1 54.2	*	2.130E+00	3.267E+00	3.737E+00	3.939E+00	4.316E+00	5.143E+00	5.363E+00	5.450E+00
-1 55.0	*	2.135E+00	3.456E+00	3.887E+00	4.136E+00	4.695E+00	5.633E+00	5.818E+00	6.114E+00
-1 55.8	*	2.112E+00	3.690E+00	4.068E+00	4.458E+00	5.277E+00	5.895E+00	6.083E+00	6.573E+00
-1 56.6	*	1.729E+00	3.154E+00	3.873E+00	4.291E+00	5.180E+00	5.629E+00	5.836E+00	6.571E+00
-1 57.4	*	1.201E+00	2.235E+00	3.364E+00	4.256E+00	4.758E+00	5.054E+00	5.292E+00	5.775E+00
-1 58.2	*	1.265E+00	1.691E+00	2.473E+00	3.220E+00	3.538E+00	3.925E+00	4.327E+00	4.871E+00
-1 59.0	*	4.005E-01	4.005E-01	4.005E-01	4.005E-01	1.588E+00	2.205E+00	2.990E+00	3.798E+00
-1 59.8	*	4.005E-01							

DECL/R.A.*	5H	39M 3.3S	39M 0.1S	38M 57.0S	38M 53.9S	38M 50.7S	38M 47.5S
-1° 51'.0	*	2.985E+00	2.223E+00	1.600E+00	1.340E+00	1.531E+00	1.627E+00
-1 51.8	*	3.907E+00	3.627E+00	3.433E+00	3.411E+00	3.094E+00	2.504E+00
-1 52.6	*	4.427E+00	4.348E+00	4.172E+00	4.313E+00	3.972E+00	3.392E+00
-1 53.4	*	4.918E+00	4.844E+00	4.645E+00	4.523E+00	4.110E+00	3.813E+00
-1 54.2	*	5.690E+00	5.496E+00	4.980E+00	4.395E+00	3.677E+00	3.405E+00
-1 55.0	*	6.209E+00	5.952E+00	5.089E+00	4.213E+00	3.464E+00	3.116E+00
-1 55.8	*	6.263E+00	5.982E+00	5.136E+00	3.915E+00	3.112E+00	2.894E+00
-1 56.6	*	6.180E+00	5.739E+00	4.496E+00	3.276E+00	2.663E+00	2.314E+00
-1 57.4	*	5.875E+00	5.222E+00	3.258E+00	2.726E+00	2.315E+00	1.836E+00
-1 58.2	*	5.147E+00	4.431E+00	2.422E+00	1.712E+00	1.468E+00	1.021E+00
-1 59.0	*	3.867E+00	2.785E+00	1.596E+00	1.059E+00	9.934E-01	9.983E-01
-1 59.8	*	4.005E-01	4.005E-01	4.005E-01	4.005E-01	4.005E-01	4.005E-01

We want to acknowledge the help of Dr. D. E. Osterbrock, Dr. A. D. Code, Dr. J. Mathis, Dr. C. Anderson, Dr. P. Pishmish, Dr. M. Méndez, Dr. M. Peimbert, Dr. S. Torres-Peimbert, Dr. P. G. Mezger, Dr. J. Schraml, Mrs. J. Valerdi, Mrs. I. Hasse and Mr. C. Schmitter. The calculations were done using the B 5500 computer at the University of Mexico Computing Center.

REFERENCES

- Boyce, P. B., 1966, *Lowell Obs. Bull.*, **6**, 215.
 Gebel, W. L., 1968, *Ap. J.*, **133**, 743.
 Ishida, K. and Kawajiri, N., 1968, *Publ. Astr. Soc. Japan*, **20**, 95.
 Johnson, H. M., 1953, *Ap. J.*, **118**, 370.
 Méndez, M., 1967, *Bol. Obs. Tonantzintla y Tacubaya*, **4**, 91.
 O'Dell, C. R., and Hubbard, W., 1965, *Ap. J.*, **142**, 591.
 Schmitter, E. F., 1971, *A. J.* (in press).
 Taylor, D. J., 1963, Ph. D. Thesis, Univ. of Wisconsin.
 Werner, M. W., Pipher, J. L., Terzian, Y., and Houck, J. R., 1969, *Ap. J.*, **155**, 485.